THE CRACK RESOLUTION REQUIRED TO ENSURE FATIGUE LIFE OF A RESCUE SUBMARINE'S TRANSFER SKIRT

M Gandomkar, Faculty of Mechanics, Malek Ashtar University of Technology, Iran
M Moshref-Javadi, Faculty of Mechanics, Malek Ashtar University of Technology, Iran

SUMMARY

Transfer skirt (TS) is a structure with spherical asymmetric sectors, which is connected to a rescue submarine and used to transfer crew between two submarines in the depth of the sea. When this structure is connected to the disabled submarine in deep, it is under violent stresses that when repeated, cause fatigue damage at sensitive regions such as welded joints. In this article, based on the Paris crack growth equation and fracture mechanics criteria in BS 7910 standard, a code is developed, by which the fatigue life of the transfer skirt structure containing various initial crack sizes is evaluated. Stress analysis is performed in order to acquire the stress distribution and to determine the stress concentration spots at the welded joints. At last, regarding the relationship between crack length and prospected life under various conditions, the minimum resolution required for examination instruments to identify defects in the welds is resolved. It seems that a permissible size of an initial crack in the welds of a transfer skirt enduring 50000 fatigue cycles is the utmost 0.65mm.

Keywords: Rescue submarine, Transfer Skirt; Fatigue; Fracture Mechanic; Crack Growth

NOMENCLATURE

a	Crack size (mm)
a_0	Initial crack size (mm)
a_c	Critical crack size (mm)
H	Operational depth (m)
v	Underwater current velocity (m s^{-1})
g	Gravity acceleration (m s^{-2})
K	Stress intensity factor ($MPa\sqrt{m}$)
σ	Stress (N m^{-2})
ρ	Density of water (kg m^{-3})
C_d	Drag coefficient
C and n	Fatigue parameters of the material
TS	Transfer Skirt
Φ	Elliptical integral function

1.   INTRODUCTION

The connecting system of a rescue submarine, called transfer skirt (TS), is a specific system that provides a dry and safe channel between a disabled and a rescue submarine to transfer crew (Stewart, 2008). This structure consists of three parts of constant, vector, and angle skirts, which are joined to each other using connecting flanges. When a rescue submarine operates under deep waters, the TS system suffers various loadings and cyclical stresses which can lead to fatigue and fracture. As well, the TS is under hydrostatic forces which may reach the yield strength, and hence, the presence of any fatigue damage which can ruin the rescue operation is probable at the susceptible zones of its structural parts. As a result, it is necessary to study the fatigue life of these structures. However, the collapse evaluations for structures operating under

external pressure in water usually cover the yield and buckling analyses (Zhang et al., 2012, Liu et al., 2014, Robles et al., 2000). Consequently, it is necessary to distinguish the fatigue sources and separately ascertain the fatigue life of the TS structure.

Figure 1 demonstrates the transfer skirt of the PRMS rescue submarine and its ABAQUS model. Also, the dimensions of a TS used in this research, inspired by the TS in Figure 1, are shown in Figure 2. The TS is made of A514 steel with a thickness of 20*mm* for its spherical hull and designed to operate at a depth of 500*m*.

Approximately, the fatigue life of a component or structure consists of two periods: crack initiation, which starts with the first load cycle and ends when a technically detectable crack is present; and crack propagation, which starts with a technically detectable crack and ends when the failure occurs. Depending on the type of component or structure, the two periods can consume widely different portions of the complete fatigue life. This is evident that if cracks or defects are present from the manufacturing steps, as is sometimes assumed for welded joints, in extreme cases, practically the whole fatigue life consists of only crack propagation (Bayley et al., 2000, Schütz, 1979).

The parts of the TS structure are connected by the welded flanges and these parts suffer dynamic forces. Therefore, it is necessary to carefully inspect the fatigue life and final fracture failure of the TS during its designing process. Besides, a precise analysis needs to consider subcritical flaw growth in the weld metal and heat-affected zones. Welded joints are more sensitive under fatigue loadings, and their fatigue life under a specific loading condition is only considered as their crack growth period. There are
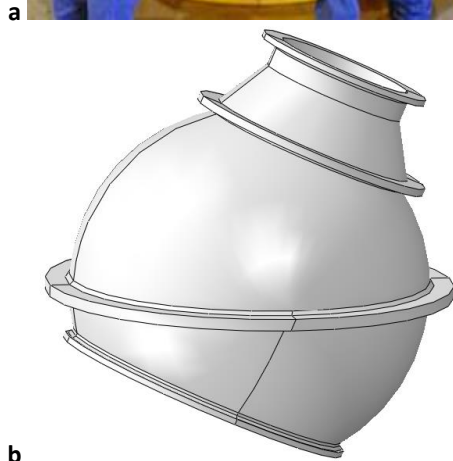
a

b

Figure 1. Transfer skirt (TS) structure, a) the TS for PRMS submarine (Wolfe and Jr., 2005), b) the drawn model in ABAQUS.
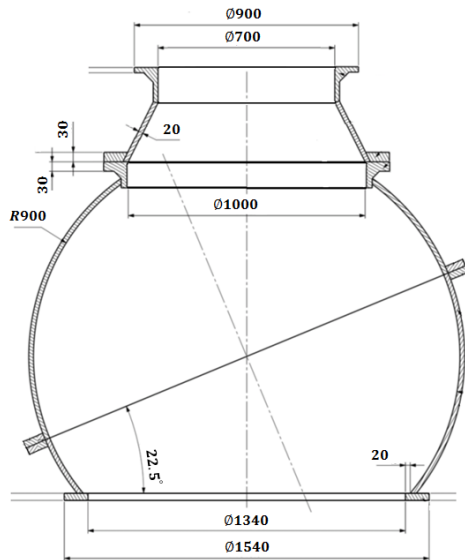

Figure 2. The dimensions of the TS used in this research (*mm*).

also many parameters such as material properties, joint configuration, stress ratio, welding instruction, welding environment, post-weld heat treatment, loading conditions, residual stresses, and reinforcement geometry that affect the fatigue behavior of the welds (Wiesner et al., 2000, Arias and Bracarense, 2017).

Two methods are utilized to predict fatigue life. The first method is based on the stress-life diagrams, and the second is according to experimental results from the fatigue tests. The later, assuming an existing crack in the structure initiated from manufacturing processes, employs fracture mechanics and crack growth methods to predict the rate of the crack growth under cyclic loadings. However, regarding that the fracture mechanics method takes relatively real assumptions and is able to realistically predict the fatigue life, this method is used here to determine the fatigue life of the TS structure (Wiesner et al., 2000, Gao et al., 2019, Wan et al., 2004).

2. FATIGUE LIFE ANALYSIS ACCORDING TO FRACTURE MECHANICS

2.1 FORCE ANALYSIS OF THE TS

Hydrostatic external pressure is the main load exerted to the TS, but other forces such as contact pressure between two mated submarines and loads caused by underwater currents are also applied to the TS system (Zhang and Wang, 2014). These forces are shown in Figure 3.
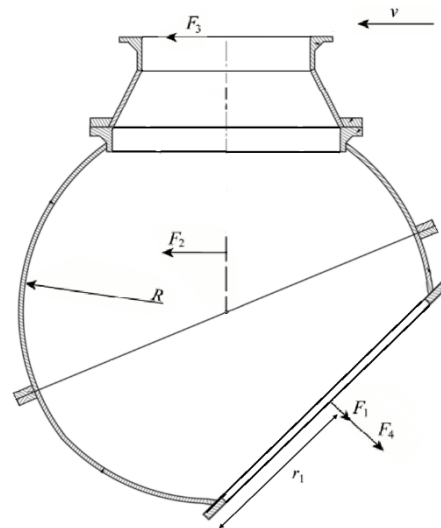

Figure 3. Modelled forces on the TS.

In this figure, *v* is the underwater current velocity; F_1, the pressure on the TS opening; F_2, the winch pull force; F_3, the forces exerted from underwater currents on the rescue submarine; and F_4, demonstrates the forces resulted from the difference between weight and buoyancy of the rescue submarine as follow:

$$F_1 = \pi r_1^2 \rho g H \qquad (1)$$

$$F_3 = \frac{1}{2} S \rho C_d v^2 \qquad (2)$$

Here, ρ is the seawater density (=1025 kg/m^3); *H*, the operational depth (=500 *m*); and *g*, the gravity acceleration. F_1 equals 9.2*kN* for the depth of 500m, and when the TS conditions are stable during operation, F_2 and F_4 forces are zero. To calculate the applied forces from the rescue submarine to the TS, the

dimensions of the rescue submarine are assumed to be 9m in length and 2m in height, which result in the side area of 18m^2. Furthermore, the drag coefficient (C_d) and v, are elected to be 1 and 1m/s, respectively, and hence, F_3 is estimated to be 10 kN according to equation (2).

2.2. FATIGUE CRACK GROWTH PARAMETERS

According to the fracture mechanics, crack growth is assumed to start from an initial size a_0 to a critical size a_c. Therefore, detection of the initial crack size in a structure is essential for the determination of the fatigue life and depends on the resolution of the inspection tool. For the safe operation of the structure during its predetermined life, first, it is necessary to extract the maximum permissible crack size according to crack growth calculations and then select the desired tool for non-destructive testing. The smallest initial crack size detected in common steel structures varies from a few hundredths to a few millimeters, depending on the accuracy of the crack detection instruments (Barter et al., 2005, Lukić and Cremona, 2001, Maddox, 1974).

It is mostly observed that the micro-cracks in the welded joints are initiated from defects at the weld toes, and joining of such micro-cracks forms almost a semi-elliptical fatigue crack (Dong and Guedes Soares, 2019). The parameter of the stress intensity factor, which is defined by the crack size and stress, is used to determine the crack growth condition according to the general equation (3) (Anderson and Anderson, 2005).

$$K = \sigma\sqrt{\pi a} \qquad (3)$$

Here, σ indicates the stress and a is the crack size. Fatigue crack growth in fracture mechanics is a function of changes in the stress intensity factor ΔK. Based on the stress intensity factor, fatigue crack growth progress is divided into three stages as indicated in Figure 4.
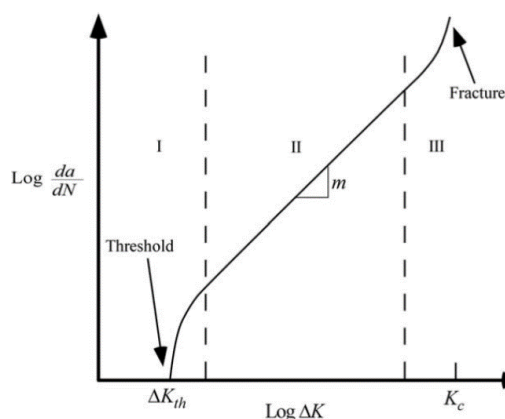

Figure 4. Diagram of the crack growth vs. stress intensity factor (Anderson and Anderson, 2005).

In stage I, where the micro-cracks present, the stress intensity factor is under the threshold value (ΔK_{th}). If ΔK for a crack is less than ΔK_{th}, the crack growth will stop

even at the macroscopic size. Stage II is the crack growth zone, where the logarithm of the crack growth shows a linear relationship with the logarithm of the stress intensity factor variations. In stage III, the crack is unstable, and the value of the stress intensity factor increases rapidly to its critical level (K_c) leading to high speed fracture failure.

According to the Paris law for stage II, the crack size development in each fatigue cycle is related to the variation of stress intensity factor by equation (4).

$$\frac{da}{dN} = C(\Delta K)^n = C(\Delta\sigma\sqrt{\pi a}\, F(a))^n \qquad (4)$$

In this equation, C and n are constants related to the intrinsic properties of the material, and $F(a)$, expressed by fatigue standards for different joint types, is a function of the shape, position, and structural location of the crack. It should be noted that there are other equations in which the effect of mean stress is also taken into account, but it is recommended to use equation (4) for steels (Wiesner et al., 2000). For welded joints subjected to periodic loads, Fricke proved that the initial cracks leading to fatigue are positioned at high-stress concentration areas and mainly at the toe and root points of the welds (Fricke, 2013). In the present study, analysis and estimation of the fatigue life for fillet welds of the TS flanges are performed according to BS 7910 standard (Standard, 2015). Table 1 and Table 2 show the mechanical properties and fatigue crack growth parameters of A514 steel plates in the air or aqueous environments and the fatigue parameters for its HAZ area, respectively. It is ideally assumed that all of the critical points have the same properties for welds and structure.

Table 1. Mechanical properties of A514 steel

	Young Modulus (GPa)	Yield Stress (MPa)	Tensile Stress (MPa)
A514 (in air and aqueous environment)	210	689	813
A514 (HAZ in air)	210	1180	1408

Table 2. Fatigue parameters of A514 steel (Yazdani and Albrecht, 1989, Committee, 1996).

	C (m/cycle)	n	ΔK_{th} ($MPa\sqrt{m}$)	K_C ($MPa\sqrt{m}$)
A514 (in air) (Yazdani and Albrecht, 1989)	2.265×10^{-11}	2.534	11.6	71.4
A514 (in aqueous environment) (Yazdani and Albrecht, 1989)	6.002×10^{-11}	2.42	12.6	64.8
A514 (HAZ in air) (Committee, 1996)	1.358×10^{-10}	2.25	--	164.7

To derive the appropriate values for the stresses in equation (4), it is necessary to divide the stress along the cross-section of the parts with high-stress concentration (in Figure 5) into two components of mean or plane stress and bending stress as following (Standard, 2015):

- Mean stress P_m: The component of stress which is uniformly developed and equals to the average stress along the cross-section. This distribution of stress must satisfy the simple law of equilibrium for internal and external forces and moments.
- Bending stress P_b: The stress component that changes linearly across the cross-section. To consider the residual stress in a conservative analysis, the residual stress may in general be assumed to be uniform and equal to the yield stress (Standard, 2015). Figure 5 schematically shows P_m and P_b variations along a structural component cross-section, in which the actual stress is linearized across the section.
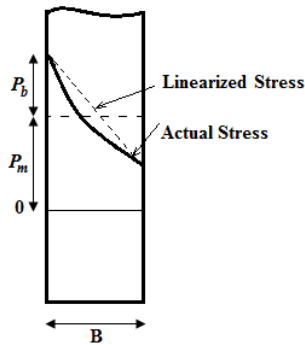

Figure 5. Schematic illustration of actual, linearized, mean, and bending stresses distributions along the cross-section of a structural part.

Considering the plate thickness of the TS in Figure 2 and assuming the width of 20*mm* for the fillet welds, a standard T-joint weld for the TS structure and the dimensions of the crack at the probable position are shown in Figure 6.
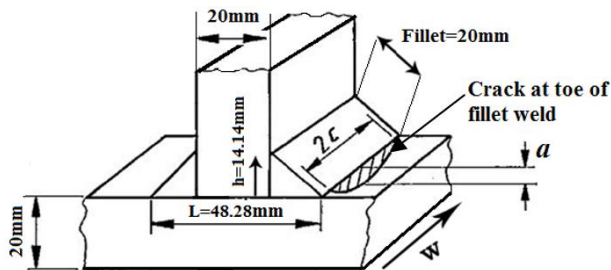

Figure 6. Dimensions of a weld joint and a crack in a fillet weld of the TS structure.

In this figure, the curvature of the TS body is neglected, but obviously, stress analysis considers the effect of body curvature. The supposed dimensions for the structure and the initial crack range needed for fatigue life analysis are shown in Table 3.

Table 3. The dimensions of the structure and the initial crack range at the toe of a fillet weld of the TS

Symbol	Description	Value (mm)
a_0	Initial depth of a crack	0.5-3
$2c_0$	Initial size of the crack opening	1-6
B	Plate thickness of the connecting flange	20
Fillet	Size of the fillet welds	20
L	Distance between two fillet welds	48.28
h	Height of the fillet weld	14.14
W	Width of the cracked plate	20

2.3 DETERMINATION OF THE STRESS INTENSITY FACTOR

The stress intensity factor of a crack is defined by the sum of the primary stress intensity factor related to the operational stresses and the secondary stress intensity factor caused by residual stress (Robles et al., 2000). According to BS 7910 standard, the stress intensity factor for elliptical cracks at the surface of a fillet weld joint under hydrostatic pressure and other forces and moments is calculated by equation (5).

$$K = \frac{\sqrt{\pi a}}{\Phi}(\sigma_m M_m M_{km} + \sigma_b M_b M_{kb}) + P\sqrt{\pi a} \qquad (5)$$

In this equation, a is the depth of the crack, σ_m the mean stress component, σ_b the bending stress component, and P is the residual stress assumed to be the material yield stress. Φ demonstrates an elliptical integral function, which is determined by the semi-elliptic shape of the crack in the fillet weld. It is proportional to the ratio of the depth-to-opening of the crack ($a/2c$) and is calculated from equation (6) (Standard, 2015).

$$\Phi = [1 + 1.464(a/c)^{1.65}]^{0.5} \qquad (6)$$

Each of the crack depth (a) or the crack opening (2c) can be detected by NDT methods; however, it is more conservative if the crack is supposed to be in its largest size. When an NDT detects a crack, the largest dimention can be considered for both (a) and (2c). Therefore, the crack depth (a) is considered as the same as the crack opening ($2c$), and both equal to the minimum resolution of the NDT instrument ($a=2c=$NDT limit).

Since the finite element analysis considers the effect of stress concentration, the M_{kb} and M_{kn} coefficients are regarded to be 1. The coefficients of mean stress (M_m) and bending stress (M_b), based on both the aspect ratio of the crack depth to the plate thickness (a/B) and the crack depth to the crack opening ($a/2c$), are obtained in accordance with standard equations for surface cracks (Standard, 2015). Because the crack depth (a) is less than 10% of the plate thickness, the standard values of M_m and M_b used in equation (6) are 0.6 and 0.65, respectively (Standard, 2015). The detectable crack size ranges from the initial size a_0 to the critical size a_c.

The standard document (Standard, 2015) states that the crack size would be acceptable if the K value is less than 0.707 K_C and the normal stress on the residual load-bearing surface is less than the yield stress (Schütz, 1979). However, the results show when the simulated maximum crack size is less than 10% of the plate thickness, there is no need to test the yield stress. It should be noted, however, that as a result of increased stress at the remained load-bearing surface in front of the crack, the steel may be subjected to plastic strain before failure.

2.4 PREDICTIVE PROCESS OF CRACK GROWTH

The predictive process of the fatigue crack growth includes the following steps that should be accomplished for each loading cycle until the crack reaches its critical size and leads to structural failure.

- Selection of the initial crack length a_0. a_0 is usually determined by the resolution of the non-destructive instrument. Besides, the initial crack opening c_0 is chosen assuming a constant ratio of ($a/2c= 1$) throughout the life of the structure. As a result, given the range of the loading stress $\Delta\sigma$, ΔK can be calculated using equation (5).
- Determining the crack growth rate of $\left(\frac{da}{dN}\right)_1$ using equation (4) in the first cycle.
- Calculating the new crack length from the equation $a = a_0 + \Delta a$ and $2c = a$.
- Steps 1 to 3 are repeated for every loading cycle to extract the crack length.

A code for the crack growth prediction was prepared in MATLAB software, and the fatigue life expectancy was extracted using the stress data from FE analysis and the crack growth relationships.

3. RESULTS AND DISCUSSION

The model was analyzed using linear and solid cubic elements (Zhang and Wang, 2014) in ABAQUS software, and the principal stresses of the TS were extracted for the depth of $500m$. It is noted that the considered stresses are the results of the unflawed structure analysis (Standard, 2015). The obtained stresses were manually compared and verified with the results of the simple static analyses at a few points away from the stress concentration regions. In Figure 8, five regions with the highest stress concentration which are susceptible to crack growth are shown.
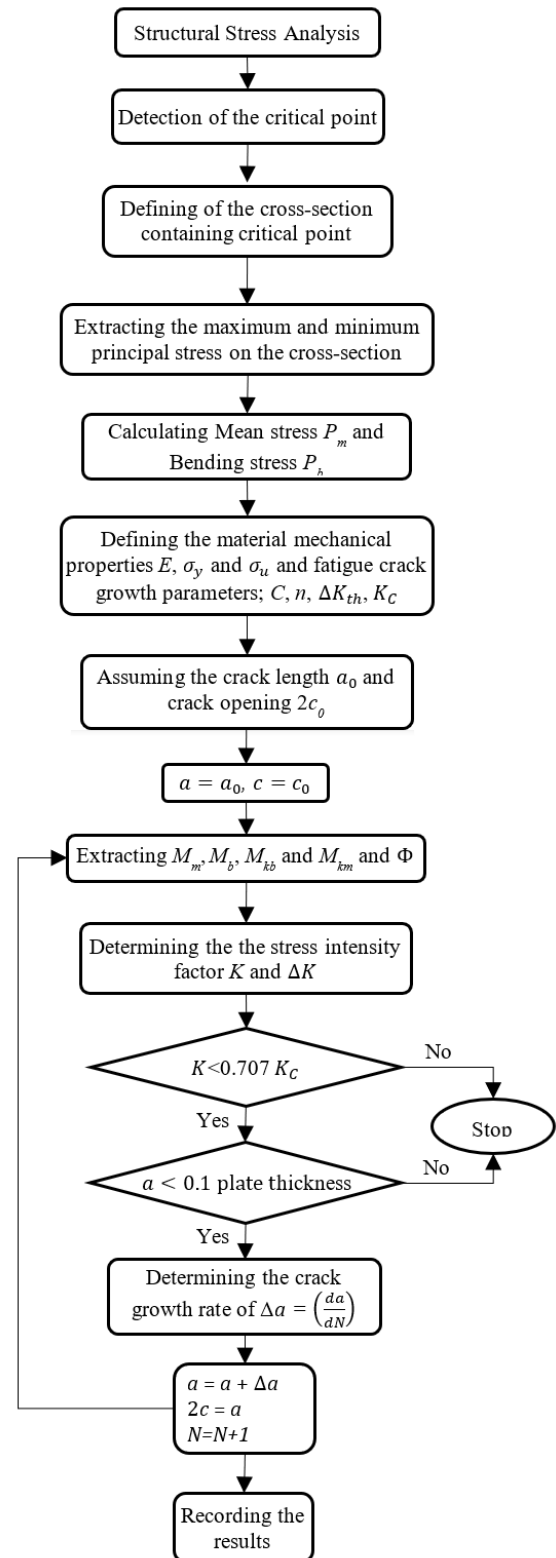

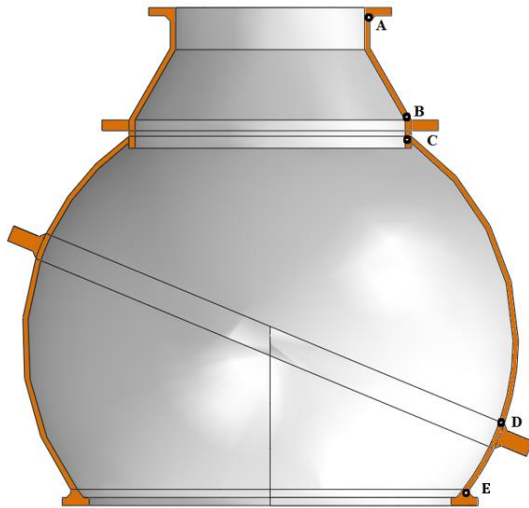Figure 7. Flowchart of the fatigue analysis process.

Figure 8. Zones susceptible to crack growth in the welded joints of the TS

In order to acquire the optimum mesh refinement or the optimum number of the elements and avoid unnecessary time and calculations, mesh convergence was performed. For five zones of A, B, C, D, and E illustrated in Figure 8, the maximum principal stresses were extracted versus element sizes. It is observed in Figure 9 that the curves of the maximum principal stresses are converging and remain horizontal after a specific element size refinement. According to the mesh convergence, 3 or 4 elements are sufficient to discretize the section thickness.
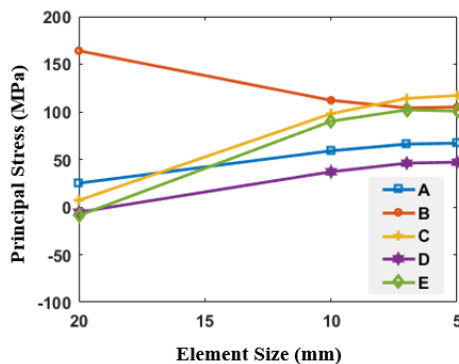

Figure 9. The convergence diagram of the stress in the five mentioned zones in figure 8.

Figure 10 depicts the maximum principal stress contours used to measure the stress intensity for these five zones. Table 4 shows the maximum and minimum of the through-thickness principal stresses extracted from ABAQUS analysis.

Table 4. The maximum and minimum through-thickness stresses for five zones of A, B, C, D, and E in Figure 7

Zone	Maximum Principal Stress (*MPa*)	Minimum Principal Stress (*MPa*)
A	65.7	-136.3
B	117.9	-322
C	121.	-295
D	59.3	-41
E	100.1	-342

According to the stress results of the five susceptible zones mentioned in Table 4, regions B, C, and E are more sensitive than others because of higher tensile principal stresses. But since the point with maximum tensile stress at zone C is not in the weld zone, this region is not critical (Hobbacher, 2016), and zones B and E are selected as the critical zones to dominate structural fatigue life. As shown in Figure 10, the maximum principal stress for zone B is 117.9*MPa* and the minimum is -322*MPa*. As a result, the mean stress is -102.1*MPa* and the maximum bending stress is 219.9*MPa*. Also, the maximum tensile stress for zone E is 99.8*MPa* and the minimum is -342*MPa*. Using these results, the mean stress is -121.1*MPa* and the maximum bending stress is 220.9*Mpa.* Moreover, the safety factor of 2 is employed on the results to determine the fatigue life.

The fatigue life determined by fracture mechanics for the fillet-weld joints of the TS in zone B is shown in Figure 11 as the crack length against the loading cycles. The minimum of the detectable initial crack length in this diagram is assumed to vary from 0.2mm to 1mm.

Depending on the position of the stress concentration, it is possible that a crack places at HAZ with higher strength than the base metal, but because of the brittle state of the HAZ, the crack grows faster. Besides, the growth speed of a crack under aqueous condition is more than that is under air condition, and if the corrosion protection is not considered properly, the crack will unpredictably grow faster. Considering that the crack growth parameters are different for the base metal and HAZ and in air and aqueous environments, it is necessary to repeat the analyses for each condition and environment using the related parameters mentioned in Table 1 and Table 2. The crack growth against the loading cycles in zones B and E considering the parameters for A514 base metal in air and aqueous environments and for its HAZ in the air environment are shown in Figures 11 and 12.

According to these diagrams, for example, when a crack with an initial length of 0.6*mm* presents in the toe of a fillet-weld of region B in the aqueous environment (Figure 10(b)), it grows to a final length of about 0.97mm after 63000 cycles, and then, the weld joint fails. Further, it is observed in Figure 10(b), that the situation exhibits the lowest fatigue life compared with other cases. As a result, the zone B and aqueous environment can be chosen as the critical position and the critical environment for crack propagation in the TS structure made of A514 steel. Besides, regarding the required life for the TS structure, the permissible initial crack length can be extracted based on the diagram of Figure 10(b), and the crack detection instrument should be selected accordingly. Consequently, depending on the performance of the TS, if 50000-cycles life is taken into account for the TS structure, it is necessary that the measurement apparatus used in the quality control stage be capable of detecting the defects with the size of at least about 0.65 mm in order to ensure that the TS structure properly operates during this number of loading cycles.
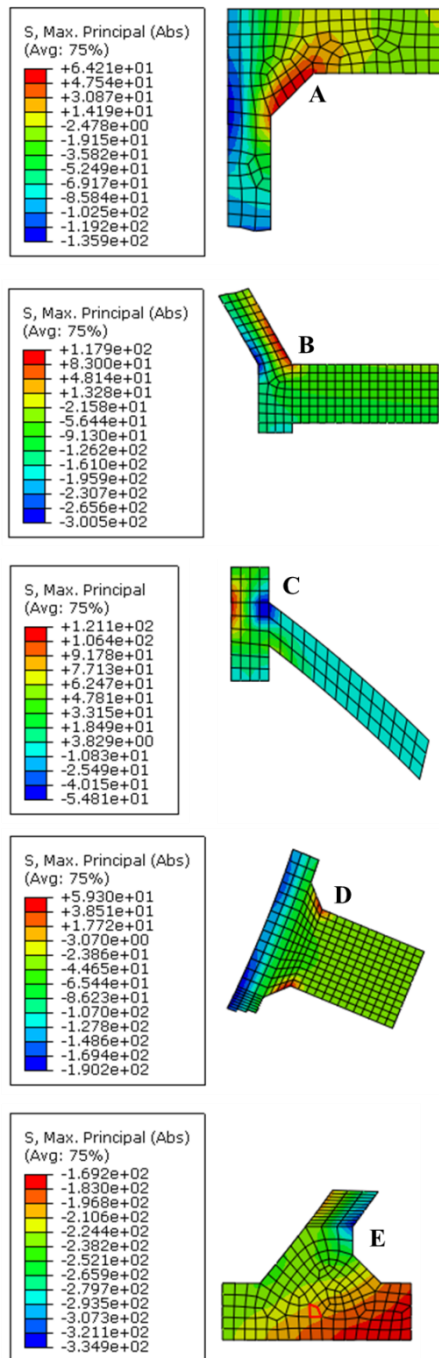
Figure 10. The contours of maximum principal stresses at five susceptible zones to crack propagation in the TS structure.

The acquired results are comparable with the typical results for the life analysis of a submarine made of HY-80 (Robles et al., 2000). The submarine has a fatigue life of 40000 cycles and its critical crack length leading to structural fracture is a_c=1.2mm. It is clear that this comparison only shows the reasonable level of the obtained results in this article for the TS structure in seawater; however, the practical conditions and the utilized materials intensively affect the final outcome.
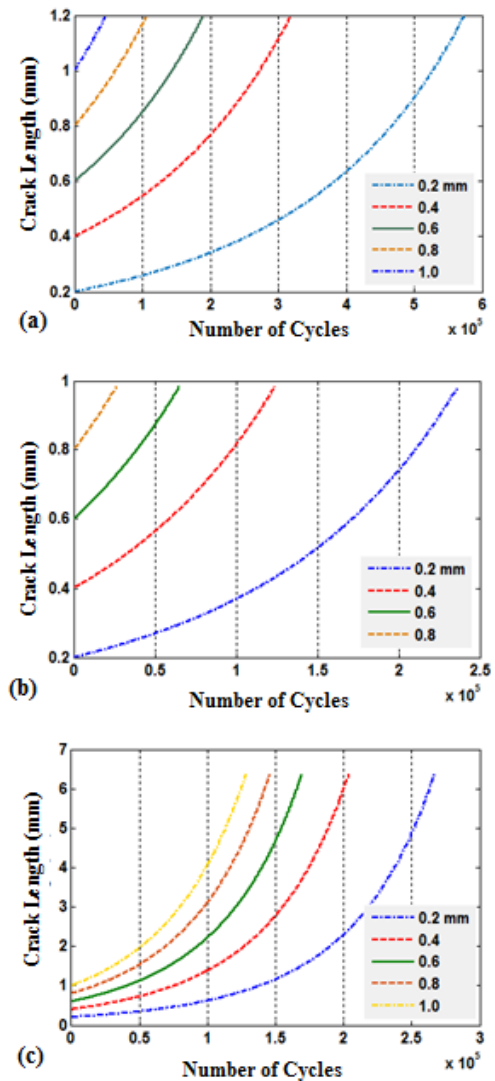

Figure 11. The diagrams of the crack growth against loading cycles in zone B with the initial crack size of 0.2mm to 1mm for A514 steel (a) in air, (b) in aqueous, and (c) for HAZ in the air environment.

4. CONCLUSION

After analyzing the TS structure and determining its sensitive regions, the stresses affecting fatigue were determined by fracture mechanics. Then, considering the welding geometry and according to BS 7910 standard, the fatigue life was determined by the Paris equation. In this respect, the different lifetimes of the TS structures were determined despite the various initial crack size. It can be concluded that the maximum initial crack size should not exceed 0.65 *mm* for 50000 fatigue cycles. Besides, the sensitive zone of the structure and critical environment for the fatigue life are distinguished to be zone B and aqueous environment.

Since the flange types and the structural stress of the TS system is similar to that of other submersible systems in which most components are at their maximum tolerance to operate at depth, fatigue analysis method for this

structure can be extended to other underwater spherical structures with openings. Therefore, these results obtained for fatigue life are also applicable to other similar spherical structures. However, since these structures are subjected to dynamic stresses, the number of dives is not equal to the number of fatigue cycles. As a result, in order to analyze the fatigue life of TS, it is necessary to modify the assumed assurance coefficient and accurately calculate the dynamic forces and the number of fatigue cycles during the TS operation.
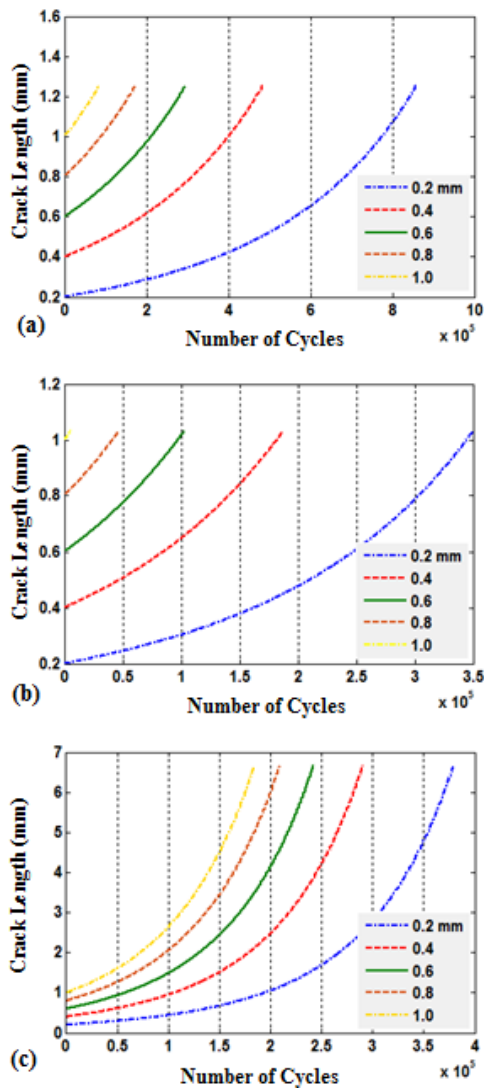

Figure 12. The diagrams of the crack growth against loading cycles in region E with the initial crack size of 0.2mm to 1mm for A514 steel (a) in air, (b) in aqueous, and (c) for HAZ in the air environment.

8. REFERENCES

1. ANDERSON, T. L. & ANDERSON, T. L. 2005. *Fracture mechanics: fundamentals and applications*, CRC press.

2. ARIAS, A. & BRACARENSE, A. 2017. Fatigue crack growth assessment in underwater wet welds. *Welding Journal,* 96**,** 287-294.

3. BARTER, S., MOLENT, L., GOLDSMITH, N. & JONES, R. 2005. An experimental evaluation of fatigue crack growth. *Engineering failure analysis,* 12**,** 99-128.

4. BAYLEY, C., GLINKA, G. & PORTER, J. J. I. J. O. F. 2000. Fatigue crack initiation and growth in A517 submerged arc welds under variable amplitude loading. 22**,** 799-808.

5. COMMITTEE, A. I. H. 1996. *ASM Handbook, Volume 19-Fatigue and Fracture*, ASM International.

6. DONG, Y. & GUEDES SOARES, C. 2019. Stress distribution and fatigue crack propagation analyses in welded joints. *Fatigue & Fracture of Engineering Materials & Structures,* 42**,** 69-83.

7. FRICKE, W. 2013. IIW guideline for the assessment of weld root fatigue. *Welding in the World,* 57**,** 753-791.

8. GAO, X., SHAO, Y., XIE, L., WANG, Y. & YANG, D. 2019. Prediction of Corrosive Fatigue Life of Submarine Pipelines of API 5L X56 Steel Materials. *Materials,* 12**,** 1031.

9. HOBBACHER, A. 2016. *Recommendations for fatigue design of welded joints and components*, Springer.

10. LIU, Y., YI, H. & CHEN, L. 2014. Submarine pressure hull butt weld fatigue life reliability prediction method. *Marine Structures,* 36**,** 51-64.

11. LUKIĆ, M. & CREMONA, C. 2001. Probabilistic assessment of welded joints versus fatigue and fracture. *Journal of Structural Engineering,* 127**,** 211-218.

12. MADDOX, S. 1974. Assessing the significance of flaws in welds subject to fatigue. *Welding journal,* 53.

13. ROBLES, L., BUELTA, M., GONCALVES, E. & SOUZA, G. 2000. A method for the evaluation of the fatigue operational life of submarine pressure hulls. *International journal of fatigue,* 22**,** 41-52.

14. SCHÜTZ, W. J. E. F. M. 1979. The prediction of fatigue life in the crack initiation and propagation stages—a state of the art survey. 11**,** 405-421.

15. STANDARD, B. 2015. BS 7910: 2013+ A1: 2015 Guide to methods for assessing the acceptability of flaws in metallic structures. *London, UK: BSI Stand Publ*.

16. STEWART, N. 2008. Submarine escape and rescue: a brief history. *Journal of Military and Veterans Health,* 17**,** 27.

17. WAN, Z., WANG, Y., BIAN, R. & ZHU, B.-J. 2004. Fatigue life prediction of structural details of submarine pres‑ sure hull. *Journal of Ship Mechanics,* 8**,** 63-70.

18. WIESNER, C., MADDOX, S., XU, W., WEBSTER, G., BURDEKIN, F., ANDREWS, R. & HARRISON, J. 2000. Engineering critical analyses to BS 7910—the UK guide on methods for assessing the acceptability of flaws in

metallic structures. *International Journal of Pressure Vessels and Piping,* 77**,** 883-893.

19. WOLFE, G. K. & JR., B. K. M. 2005. Voyage from the Bottom of the Sea SwRI researchers help design a next-generation submarine rescue vehicle. *Technology Today,* 27**,** 2-7.

20. YAZDANI, N. & ALBRECHT, P. J. E. F. M. 1989. Crack growth rates of structural steel in air and aqueous environments. 32**,** 997-1007.

21. ZHANG, Z. L. & WANG, L. Q. The Research on Shell Strength and Pressurize Reliability of Underwater Vehicle Mating Device. Key Engineering Materials, 2014. Trans Tech Publ, 197-200.

22. ZHANG, Z. Y., SONG, T. S. & HE, Y. Fatigue Life Reliability Analysis of Submarine Cone-Cylinder Shell. Advanced Materials Research, 2012. Trans Tech Publ, 2001-2004.